Full-Body Cardiovascular and Tumor MRI for Early Detection of Disease: Feasibility and Initial Experience in 298 Subjects

Susanne C. Goehde[1]
Peter Hunold
Florian M. Vogt
Waleed Ajaj
Mathias Goyen
Christoph U. Herborn
Michael Forsting
Jörg F. Debatin
Stefan G. Ruehm

OBJECTIVE. High diagnostic accuracy, emerging whole-body concepts, and lack of side effects combine to render MRI a natural candidate for screening purposes. The aim of this study was to evaluate the technical feasibility of a comprehensive multiorgan-targeting MRI examination and determine the frequency of findings in subjects without a history of serious disease.

SUBJECTS AND METHODS. The study group was composed of 331 subjects. The MRI protocol (mean examination time, 63 min) encompassed the target organs: the brain, arterial system, heart, and colon. Diagnoses were deemed relevant if the physician had to inform the subject about the findings. Subjects with a history of serious illnesses were excluded from subsequent analysis (n = 33). All analyses were performed for the resulting subgroup of 298 subjects (247 men, 51 women; mean age, 49.7 years).

RESULTS. All 298 examinations were diagnostic excluding eight MR colonography components in which remaining stool hampered reliable diagnosis. Follow-up or radiologic confirmation could be obtained in 75% of all cases with relevant findings (128/169); only one false-positive result was encountered. Of the study group, 21% exhibited signs of atherosclerotic disease. Two cerebral infarctions and one myocardial infarction, previously unknown, were encountered; 12% had peripheral vascular disease. Twelve colonic polyps and nine pulmonary lesions were correctly detected. Of all MRI examinations, 29% revealed relevant additional findings in nontargeted organs. Only one minor allergoid reaction was encountered.

CONCLUSION. The presented data point toward an increased use of MRI for screening in the future, but to date screening MRI should not be performed outside a research setting because the cost–benefit relation is unclear.

The use of radiologic imaging is generally focused on detecting and characterizing suspected or known disease in symptomatic patients. Experience with screening, aiming at the detection of disease before its symptomatic manifestation, is limited. Recently, the use of MDCT has been suggested for screening. Driven by dramatic increases in scanning speed, early manifestations of cardiovascular disease [1] and lung [2–4] and colon [5] cancer are being targeted with this technology.

Risks associated with high radiation doses inherent to CT cast a shadow on the future of CT-based screening. Although with recent low-dose protocols the total radiation dose to the subject is minimized and radiation-induced individual risk might be far less than the risk of subsequent diagnostic and therapeutic interventions, the U.S. Food and Drug Administration has issued radiation alerts [6], and the European Union has passed legislation prohibiting the use of examinations based on ionizing radiation for screening purposes except mammography [7]. Recognition thereof has focused attention on an imaging technique void of ionizing radiation or other harmful side effects: MRI.

On the basis of the inherently high soft-tissue contrast in conjunction with high spatial and temporal resolution, MRI emerged as the imaging technique of choice in the evaluation of many organs. Among them, the central nervous system features prominently; inflammatory, neoplastic, and vascular disease are reliably detected or excluded using MRI [8, 9].

Similarly, the arterial system is accurately assessed with MR angiography. Compared with catheter-based angiography, MR angiography has been shown to be equivalent in virtually all territories including the carotid [10], renal [11], and peripheral [12] arteries. Moti-

Received May 19, 2003; accepted after revision June 30, 2004.

[1]All authors: Department of Diagnostic and Interventional Radiology, University Hospital Essen, Hufelandstrasse 55, Essen 45122, Germany. Address correspondence to S. C. Goehde.

AJR 2005;184:598–611

0361–803X/05/1842–598

© American Roentgen Ray Society

TABLE 1 Parameters of the Four MR Examination Parts

Parameter	Head (Axial)					Heart and Lungs					Arteries and Colon (Coronal)	
	2D T1 Spin-Echo	2D T2 Turbo Spin-Echo	3D Gradient Echo Time of Flight	2D Inversion Recovery FLAIR	Diffusion-Weighted Echo-Planar Imaging	2D HASTE Axial	2D Cine Long Axes	2D Cine Short Axis Shared Phases	2D Inversion-Recovery/FLASH Long-Axis Late Enhancement	3D Inversion-Recovery/FLASH Short-Axis Late Enhancement	3D FLASH MR Angiography	3D FLASH MR Colonography (VIBE)
Field of view (mm^2)	19 × 23	19 × 23	19 × 23	19 × 23	19 × 23	Dependent on patient size	Dependent on patient size	Dependent on patient size	Dependent on patient size	Dependent on patient size	Dependent on patient size	Dependent on patient size
Matrix	256 × 167	256 × 167	512 × 192	256 × 198	256 × 198	256 × 117	256 × 179	256 × 179	256 × 179	256 × 192	256 × 220	168 × 256
TR (msec)	204	4,300	40	8,430	3,400	800	45	45	690	700	2.2	3.1
TE (msec)	4.8	105	7.2	162	118	22	1.5	1.5	4.4	1.49	0.74	1.1
Inversion time (msec)				2,500					150–250	150–250		
Flip angle (°)	90	90	25	150	90	160	60	60	25	10	20	12
Slice thickness (mm)	7.2	7.2	1.0	7.2	7.2	10.4	8	5	8	5	1.8 (× 64)	1.8 (× 96)
Spectrospatial fat saturation	0	0	0 3 slabs	0	Yes b 0, b 500, b 1,000	0	0	0	0	0	0	Yes
Injection (mL)											0.2 mmol/kg diluted with saline to 60 mL	
Injection speed											Biphasic: 1) 30 mL at 1.2 mL/sec 2) 30 ml at 0.7 mL/sec plus saline flush	0.1 mmol/kg at 1.2 mL/sec
T delay											Individual bolus timing in aortic arch	"Native," 60sec, 90sec

Note.—Given values are approximate numbers (depends on patient thickness, heartbeat rate, and so on). FLASH = fast low-angle shot, VIBE = volumetric interpolated breath-hold examination. FLAIR = fast low-angle inversion recovery sequence; HASTE = half-Fourier acquisition single shot turbo spin-echo sequence.

vated by the systemic nature of atherosclerotic disease, the concept of whole-body MR angiography—encompassing the arterial tree from the carotids to the trifurcation vessels—has recently been introduced [13].

At the same time, cardiac MRI permits the evaluation of regional and global myocardial contractibility, valvular function [14], and myocardial viability and perfusion [15]. Finally, MRI has been shown to be capable of detecting mass lesions exceeding 10 mm in the lungs [16] and colon [17] with high sensitivity and specificity.

To date, cost concerns and lengthy data acquisition times have prohibited the use of MRI for screening. Recent hard- and software advances combining toward faster data acquisition over several body regions have opened new possibilities. Thus, a comprehensive 60-min MRI protocol permitting the detection of early cardiovascular disease and lung and colon cancer has been developed. The purpose of this study was to assess the technical feasibility of this MRI-based comprehensive screening strategy and to determine the frequency of findings pointing to the targeted and other diseases.

Subjects and Methods

Subjects

Over a 15-month period (July 2001–September 2002) a comprehensive MRI examination was performed on 331 adults who ranged in age from 31 to 81 years (mean age, 50.2 years). The study was conducted in accordance with the ethical standards of the local institutional committee on human experimentation. The subjects were recruited from corporations offering preventive health care programs to employees. The subjects did not receive any compensation for participation. Written informed consent was obtained from all participants, who were not charged for the examination. The study character of the MRI examinations was explained, and it was stated explicitly that this MRI examination can to date not replace any other screening test. The possibilities and limitations were explained—for example, that the heart examination cannot depict the coronary arteries. Subjects with contraindications to MRI (n = 1) were excluded previously; the total number of MRI examinations performed thus was 331. No case of claustrophobia occurred. Subjects with known serious illnesses including myocardial infarction (n = 2), stroke (n = 2), malignant tumors (n = 17), or diabetes mellitus (n = 12) were identified by questionnaire and excluded from the subsequent analysis.

Subsequent analysis was thus limited to a subgroup of 298 subjects encompassing 247 men and 51 women who ranged in age from 31 and 73 years

with a mean age of 49.7 years. Only 2.6% of them were 65 years old or older, and only 15.8% were under 40 years old. Of the group, 20% were smokers, and the mean body mass index was 24.6. The imaging material was shown to the subjects after completion of the examination. Compliance regarding suggested treatment or follow-up diagnostic examinations was monitored by telephone interviews and review of medical records.

MRI

Imaging was performed on a 1.5-T MRI system (Magnetom Sonata, Siemens Medical Solutions), equipped with a fully MRI-compatible rolling table platform (Angio*SURF*, MR-Innovation) for whole-body coverage [18], which allows image acquisition using a body array surface coil. The comprehensive MRI-based screening protocol contained five components (Tables 1 and 2).

First, the cerebrum was assessed by fast T1- and T2-weighted spin-echo, FLAIR, and diffusion-weighted imaging. The intracerebral arterial system was directly visualized by axial 3D time-of-flight MR angiography. At a later time point (after the cardiac examination), a T1-weighted gradient-echo sequence was applied, which made use of the contrast agent that had been given for MR angiography (contrast-enhanced sequence of the brain for tumor detection). This sequence was performed for subject number 51 and all subsequent examinations; before this time point, the contrast-enhanced sequence was not part of the protocol.

Second, whole-body MR angiography based on the acquisition of five slightly overlapping 3D coronal data sets (64 sections each) acquired in immediate succession using a fast 3D fast low-angle shot (FLASH) sequence was performed. Each data set was collected over 12 sec, and the first three data sets were acquired using the breath-hold technique. The addition of a 3-sec pause for table movement from one body region to the next translates into a total acquisition time of 72 sec. After conventional test bolus timing with 1 mL at 1.2 mL/sec for individual assessment of circulation time, a 1-molar gadolinium-based contrast agent (Gadobutrol, Gadovist 1.0, Schering) was administered at a dose of 0.2 mmol/kg of body weight for arterial enhancement [19, 20] via a 19-gauge plastic IV line placed in the antecubital vein. The contrast material was diluted with saline solution to a total amount of 60 mL. Then, a biphasic contrast injection protocol was used: a first flush of 30 mL at 1.2 mL/sec and a second flush at 0.7 mL/sec, followed by a saline flush of 20 mL at 0.7 mL/sec. No venous compression was used.

Axial HASTE imaging (slice thickness, 8 mm) of the thorax was performed to depict the pulmonary parenchyma and cardiac morphology. For this purpose, two blocks of slices were acquired, both using the breath-hold technique. The former injected contrast agent (for MR angiography) does not alter the value of this T2-weighted sequence. No additional contrast material was given for this MRI examination of the lungs.

Subsequent functional assessment of the heart was based on segmented true fast imaging with steady-state free-precession (true FISP) cine measurements collected in the left ventricular short axis. Standard valvular views (four-chamber, two-chamber, and outflow) were added. A segmented inver-

TABLE 2 Time Course of the MRI Examination

Organ	Order of Sequences	Signal Reception	Contrast Injection	Total Examination Time (min)
Head	T1-weighted	Head coil	0	10
	T2-weighted		0	
	FLAIR		0	
	Diffusion-weighted		0	
	Time-of-flight		0	
Arteries	Bolus timing	Body array and spine surface coil with moving table AngioSURF[a]	2 mL at 1.2 mL/sec	15
	3D FLASH coronal		0.2 mmol/kg of body weight of a 0.5 molar gadolinium-based MR contrast agent were diluted with saline to 60 mL. First 30 mL injected at 1.2 mL/sec, second 30 mL injected at 0.7 mL/sec	
	1) Supraclavicular			
	2) Thorax			
	3) Abdomen and pelvis			
	4) Upper legs			
	5) Lower legs			
Heart	HASTE	Body array coil and spine array coil	0	15
	2D cine 4-chamber view		0	
	2D cine 2-chamber view		0	
	2D cines short axis		0	
	2D inversion-recovery FLASH late enhancement 4-chamber view		0[b]	
	2D inversion-recovery FLASH late enhancement 2-chamber view			
	3D inversion-recovery FLASH late enhancement short axis (x 2 for whole coverage)			
Colon	Bowel cleansing	Body array coils and spine array coil	40 mg scopolamine at time of enema; 1,500–2,000 mL of water enema	10
	3D FLASH (VIBE)		0	
	1) "Native"			
	2) 60 sec after injection		0.1 mmol/kg of body weight at 1.2 mL/sec	
	3) 90 sec after injection			

Note.—Between each examination part, coil settings are changed. Contrast agent is administered at two occasions: angiography and colonography. FLASH = fast low-angle shot, VIBE = volumetric interpolated breath-hold examination.

[a]MR-Innovation.

[b]Makes use of contrast material injected at MR angiography.

TABLE 3 Results of the Questionnaire (*n* = 331)

Clinical Data	No. of Patients
Known arterial hypertension	54
Malignancy in history	17
Diabetes mellitus	12
Stroke	2
Myocardial infarction	2
Present actual medication	128

sion recovery turbo gradient-echo sequence, collected in both the short (3D) and long (2D) axes making use of the contrast administration for whole-body MR angiography, was assessed for areas of late enhancement denoting myocardial infarction. A total of 13–18 breath-holds were performed.

For MR colonography, all subjects had undergone standard preparation for bowel cleansing. Scopolamine (40 mg) was administered IV to minimize bowel motion. Glaucoma required the alternative use of glucagon in three subjects (dosage 100 mg = 1 IU). The subjects were imaged in the prone position only because air bubbles, due to their low signal, do not pose a problem in image assessment of the T1-weighted sequences. The colon was filled with 1,500–2,500 mL of warm tap water via rectal enema. The amount of water administered rectally was chosen according to the subject's acceptance. No fluoroscopic imaging was performed for guidance of the enema, because our experience shows that this approach results in sufficient colonic distention. T1-weighted 3D gradient-echo images (96 sections) of the colon were collected during breath-holding over 23 sec before and 60 and 90 sec after a second IV administration of gadobutrol at a dose of 0.1 mmol/kg of body weight.

Imaging Data Review

The in-room time—that is, the time between the subject entering the MRI room for positioning and the subject leaving the MRI room—was determined. All imaging data were analyzed prospectively on a workstation (Virtuoso, Siemens Medical

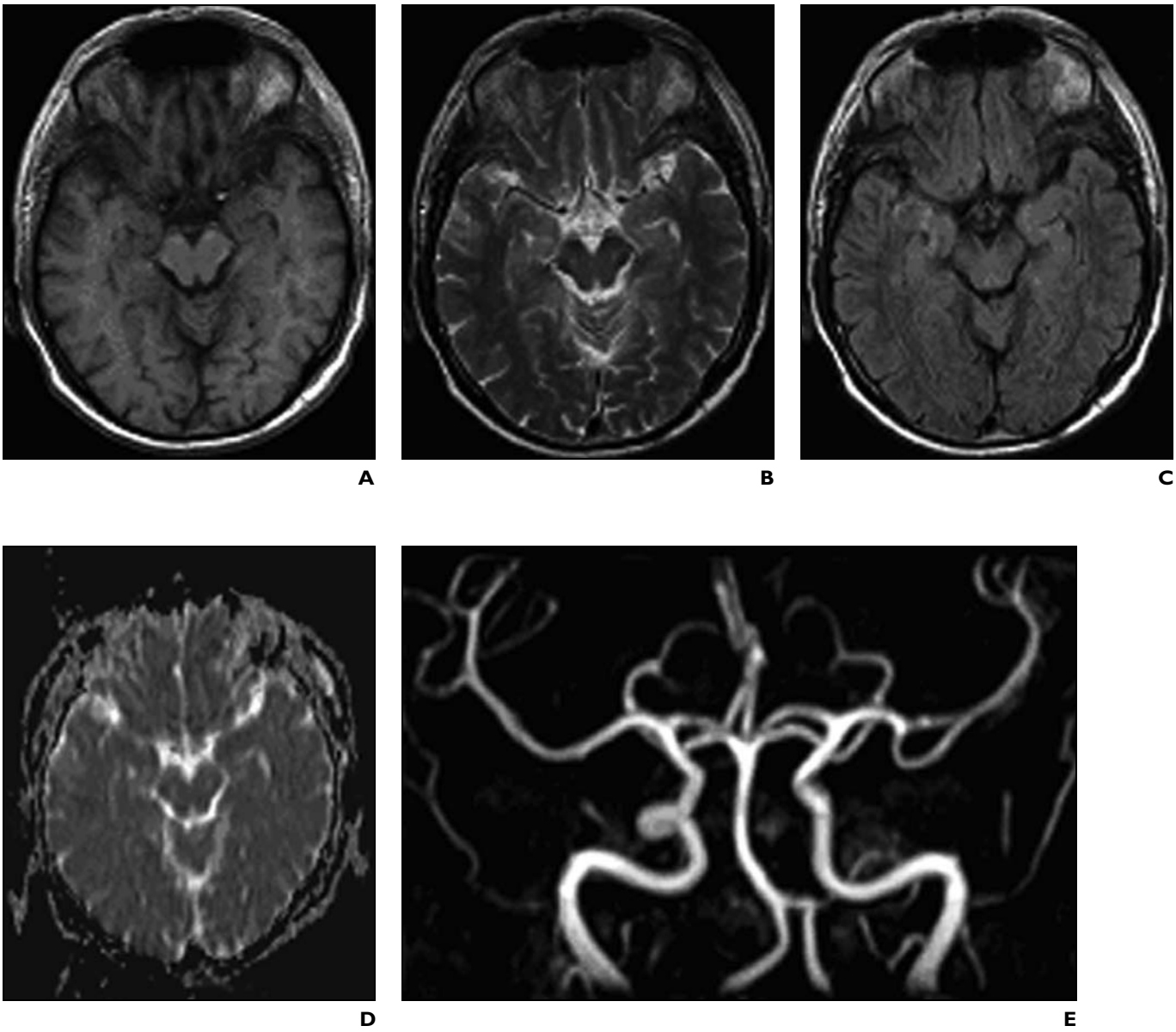

Fig. 1.—51-year-old male smoker with hyperlipidemia (same subject as in Figs. 2–5). MRI assessment of brain can be completed within 10 min.
A–C, MR images of brain parenchyma show normal findings: T1-weighted FLASH image (**A**), T2-weighted turbo spin-echo image (**B**), and FLAIR image (**C**).
D, Diffusion-weighted image reveals normal function.
E, Time-of-flight image shows that arterial morphology is normal.

Solutions) and interpreted by two board-certified radiologists with extensive MR experience (> 5 years) in consensus. The workstation permitted 2D, 3D, and cine loop viewing and rendered maximum intensity projections and multiplanar reformations. The reviewers were privy to the questionnaires filled out by the subject before the examination.

MRI data of the brain were reviewed for the presence of direct or indirect signs of vascular disease as evidenced by alterations affecting the intracerebral arteries themselves or the cerebral parenchyma (infarction, white matter lesions). Additional findings within the brain or other structures such as the paranasal sinuses were also noted.

Whole-body MR angiography was analyzed for the presence of arterial luminal narrowing exceeding 50% on the basis of the most severe reduction of the arterial diameter compared with the most normal-appearing segment proximal or distal to the area of arterial compromise, arterial occlusion, arterial wall irregularities, ectasia of vessel parts, and aneurysmal disease. For this purpose, no image mask subtraction was used in any of the five angiography stations.

MRI data of the heart were reviewed qualitatively according to the following diagnostic groupings: myocardial infarction (transmural or nontransmural), regional wall motion disorders, global contractibility reduction, myocardial hypertrophy, and valvular disease. In case the diagnosis of a potentially reduced global ejection fraction was made, a subsequent quantitative analysis of the respective parameters (end-systolic and end-diastolic volume, ejection fraction) was performed using semiautomatic cardiac evaluation software (Argus, Siemens Medical Solutions).

The pulmonary parenchyma was evaluated for the presence, location, and size of pulmonary mass lesions and other incidental findings such as pleural effusions.

Similarly, MR colonography data sets were searched for the presence of enhancing colorectal masses. Reported incidental findings included diverticular disease and renal, hepatic, spinal, adrenal, gastric, pancreatic, and retroperitoneal masses.

Data Analysis

Findings were characterized as relevant or not relevant. Relevant findings led to informing the subject of the findings, a therapeutic recommendation, or mandated subsequent diagnostic follow-up. This definition was used according to the routine clinical setting, in which nonmalignant findings are also explained in the reports or, in case of self-referral, in which the subjects are informed about possibly important findings. This includes anatomic variations such as the retroaortic renal vein or degenerative spine disease because these findings can lead to symptoms and hepatic hemangiomas because this finding might pose differential diagnostic problems in the future; the informed patient can resolve the problem.

Thus, arterial narrowing exceeding 50%; the presence of aneurysmal disease, cerebral infarctions, or extended microangiopathic white matter lesions; colorectal masses; and evidence of myocardial infarction, reduced regional or global ventricular wall motion, left ventricular hypertrophy, and valvular disease were considered relevant. Similarly, the presence of gastric herniation, renal masses, focal pulmonary lesions of potential malignancy, extensive paranasal sinusitis, heterogeneous or enlarged thyroid, adrenal masses, and frank spinal disk herniation were considered relevant. Identification of renal or hepatic cysts or hemangiomas and of light to moderate paranasal sinusitis was considered not relevant. Similarly, focal arterial irregularities or stenoses with luminal narrowing of less than 50% and diverticular disease were considered not relevant.

Results

Except for one minor allergoid reaction (skin rash) after the administration of paramagnetic contrast material, all 331 subjects tolerated the comprehensive MRI examination well. The mean in-room time for all subjects was 63 min and ranged from 54 to 85 min. In one subject, a technical problem led to reduced but diagnostic contrast within the supraaortic vessels. In two subjects, the body array surface coil could not be used for MR angiography; in these cases, image acquisition was performed using the integrated body coil, leading to a reduced signal-to-noise ratio; however, the images were of sufficient image quality for this study. Cardiac imaging revealed no image quality loss due to arrhythmia. All remaining components of the comprehensive MRI examination were considered diagnostic in all subjects.

Subsequent disease-oriented analysis was limited to the 298 subjects who were considered not seriously ill. Results of a cursory questionnaire focusing on medical history are summarized in Table 3. Only 69% of all subjects did not show any relevant finding in the target organs (arteries, heart, brain, or colon) (Figs. 1–5).

Vascular Disease

Of the 298 subjects, MRI revealed signs of cerebrovascular, peripheral vascular, or cardiovascular disease in 21% (Table 4). Twenty-seven subjects (9%) had unequivocal macro- or microangiopathic changes within the cerebrovascular system, nine of them of medium to higher degree (Table 4 and Fig. 6).

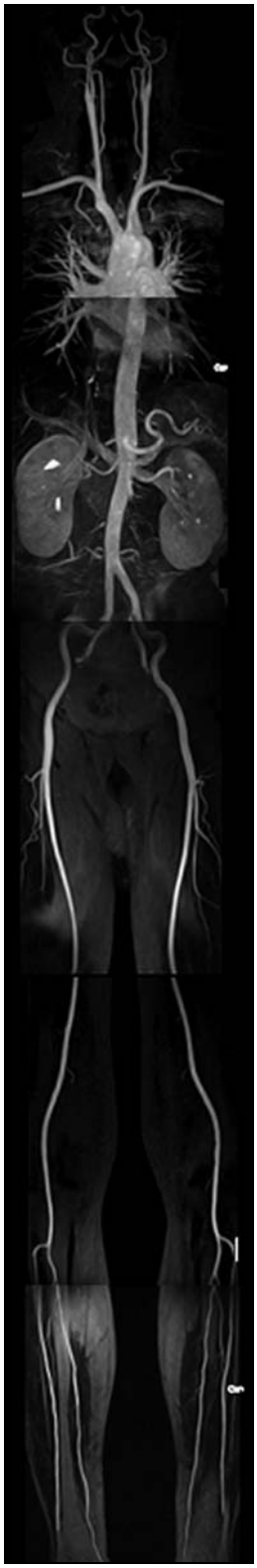

Fig. 2.—51-year-old male smoker with hyperlipidemia (same subject as in Figs. 1 and 3–5). Whole-body angiogram (data acquisition time, 72 sec) shows normal findings.

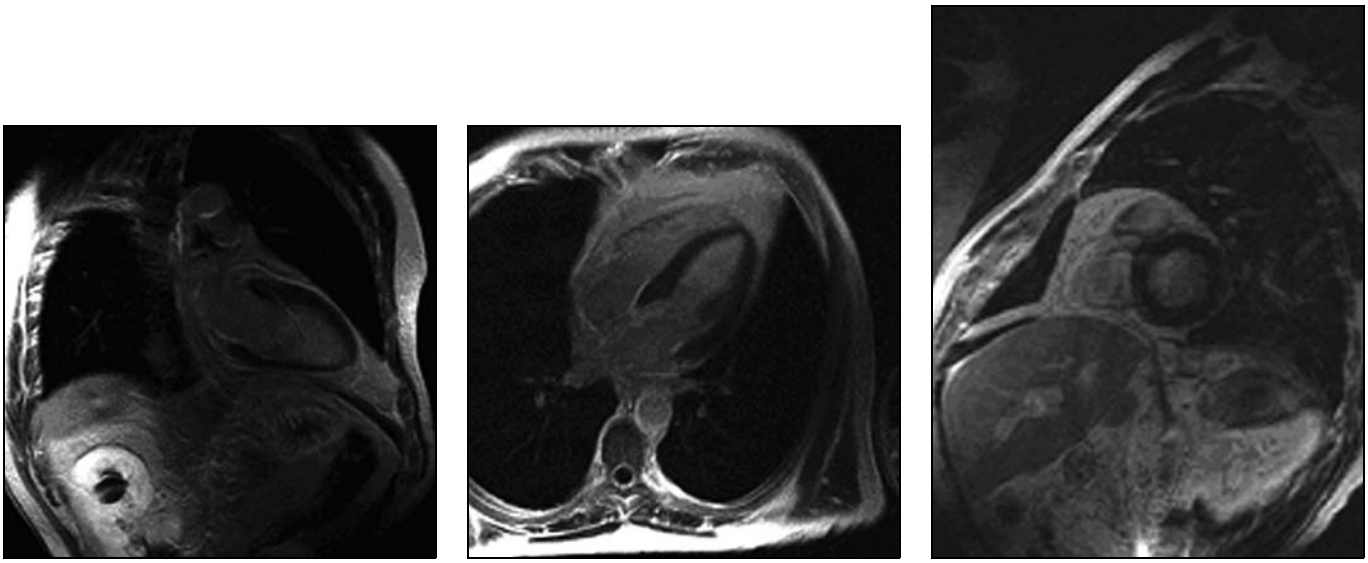

Fig. 3.—51-year-old male smoker with hyperlipidemia (same subject as in Figs. 1, 2, 4, and 5).
A–C, Two-chamber (**A**), four-chamber (**B**), short-axis (**C**) views show normal late enhancement study of heart.

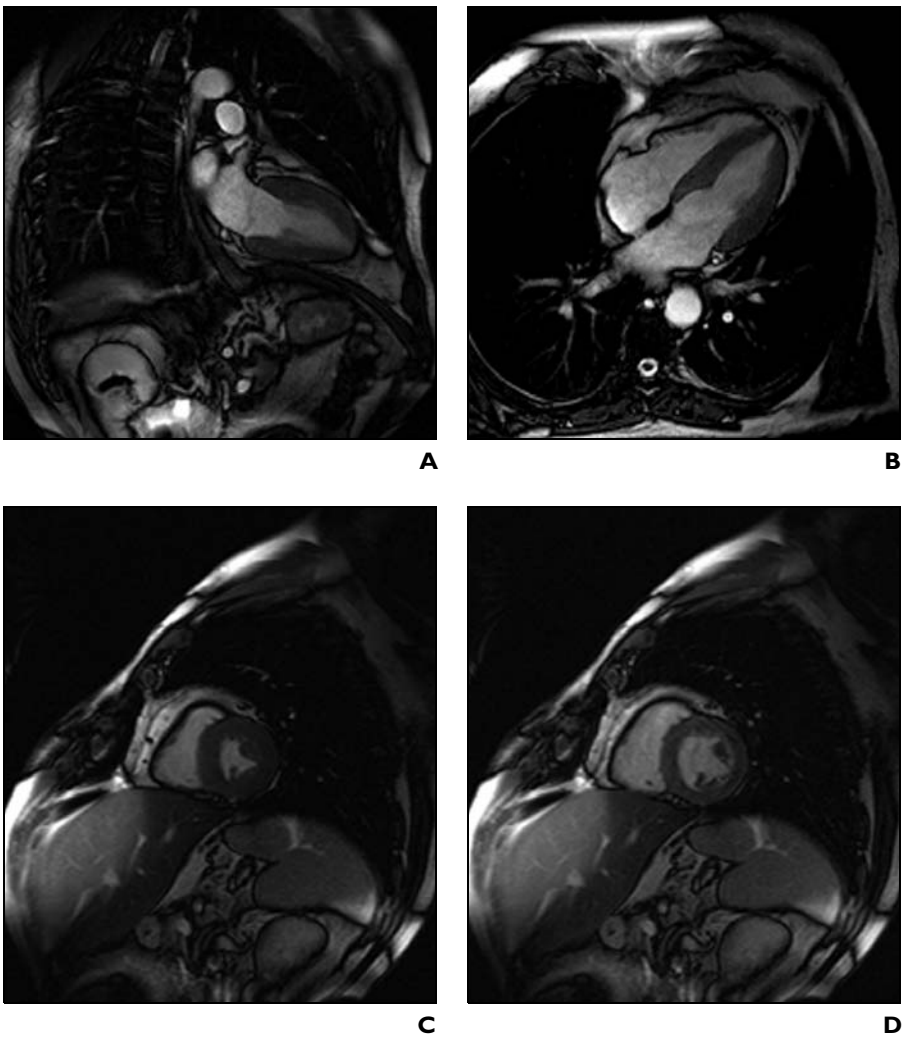

Fig. 4.—Steady-state free precession (trueFISP) cine of the heart in 51-year-old male smoker with hyperlipidemia (same subject as in Figs 1–3 and 5).
A–D, Two-chamber view obtained during systole (**A**), four-chamber view obtained during systole (**B**), short-axis view obtained during systole (**C**), and short-axis view obtained during diastole (**D**) show normal findings.

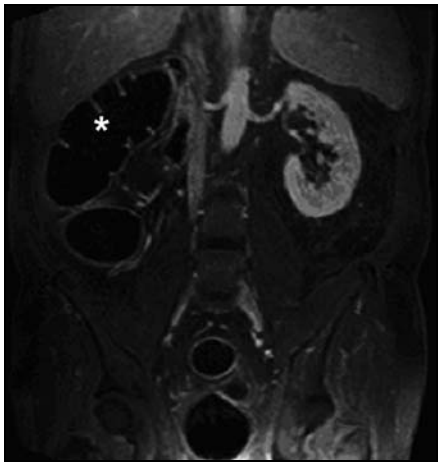

Fig. 5.—51-year-old male smoker with hyperlipidemia (same subject as in Figs. 1–4). Source MR colonography image from 96-slice 3D coronal gradient-echo data set, acquired 60 sec after IV contrast injection shows normal findings (acquisition time, 24 sec). Rectal enema with water renders colonic lumen (*asterisk*) dark.

TABLE 4 Relevant Findings with Regard to the Target Diseases Atherosclerosis and Colonic Polyps as Well as Lung Nodules

Technique	Main Findings on MRI	Relevant Findings (*n*)	Confirmation of Relevant Findings	Nonrelevant Findings (*n*)
Cerebral MRI	Tandem ICA stenosis	1	Duplex sonography	
	Plaque of ICA	1	Duplex sonography	
	Unknown cerebral infarctions	2	Dedicated MRI	
	Microangiopathic changes	5	None	18
	Sum	9		18
MR angiography	Focal dissection of SFA	1	Duplex sonography	
	Plaque of ICA	2	Duplex sonography	
	Stenosis > 50% of ICA	2	Duplex sonography	
	Focal dissection of infrarenal aorta	1	CT angiography	
	Renal artery stenosis	1	Sonography	
	Aneurysm of ascending aorta > 4 cm	1	None	
	Infrarenal aortic aneurysm > 4 cm	2	Sonography	
	Plaques or wall irregularities	6	None	10
	Lower limb artery stenoses	3	Sonography (*n* = 2)	
	Plaque at CCA or vertebral artery		None	2
	Elongation of aorta or great vessels		None	5
	Iliac artery stenosis	1	Sonography	
	Total	20		17
Pulmonary MRI	Benign lesions		CT: 4 lesions in two subjects with most probably benign lesions confirmed (nonrelevant), in two subjects a CT control was not available	4
	Suspicious lesions	1	No control available	
	Total	1		4
Cardiac MRI	Reduced global or regional contraction	5	Echocardiography	
	Myocardial infarction	1	Dedicated MRI	
	Total	6		
MR colonography	Unequivocal polpys	12	Polypectomy	
	Remaining stool		Dedicated MR colonography	3
	Total	12		3

Note.—List of target diseases (atherosclerotic findings, pulmonary lesions, and colonic polyps) of 298 subjects. *n* = number of subjects with respective finding, ICA = internal carotid artery, SFA = superficial femoral artery, CCA = common carotid artery.

Of those, MRI revealed unknown cerebral infarctions in two subjects and a tandem stenosis of the extracranial internal carotid artery in one subject.

In 20 subjects (7%), whole-body MR angiography revealed relevant signs of atherosclerosis (Table 4), including two high-grade stenoses of the proximal internal carotid artery, a focal dissection of the infrarenal aorta in a 40-year-old smoker, and dissection of the superficial femoral artery in a 52-year-old smoker (Fig. 7). In two subjects, one intracerebral aneurysm (size, 5 mm) and one fenestration of the basilar artery were detected as a risk factor for the development of cerebral aneurysms. In 18 additional individuals, only irregularities of the vessel walls or focal calcified plaques of the peripheral arterial system were identified; those cases with multifocal extended atherosclerotic disease or plaques of the internal carotid artery (n = 8) were regarded as relevant.

No subject had difficulties performing the repeated breath-holds (up to 18) during the cardiac part of the examination. Cardiac MRI revealed a previously unknown subendocardial infarction in a 62-year-old man, shown by late enhancement. In five individuals, all men, regional or global myocardial dyskinesia with reduced ejection fractions (< 50%) was noted. MRI revealed left myocardial hypertrophy in 17 subjects, of those 64.7% had known arterial hypertension, compared with only 23.8% of the remaining subjects. Eleven subjects had valvular disease.

Pulmonary Disease

The HASTE data sets revealed nine pulmonary lesions ranging in diameter between 3 and 7 mm in five subjects. Of those, seven were classified as probably benign, making use of a set of different parameters such as signal, size, and shape. CT was performed for further evaluation in only of two subjects (each with two pulmonary lesions); in these cases, the lesions could be confirmed to be benign (Fig. 8) and the single masses were found to be partially calcified.

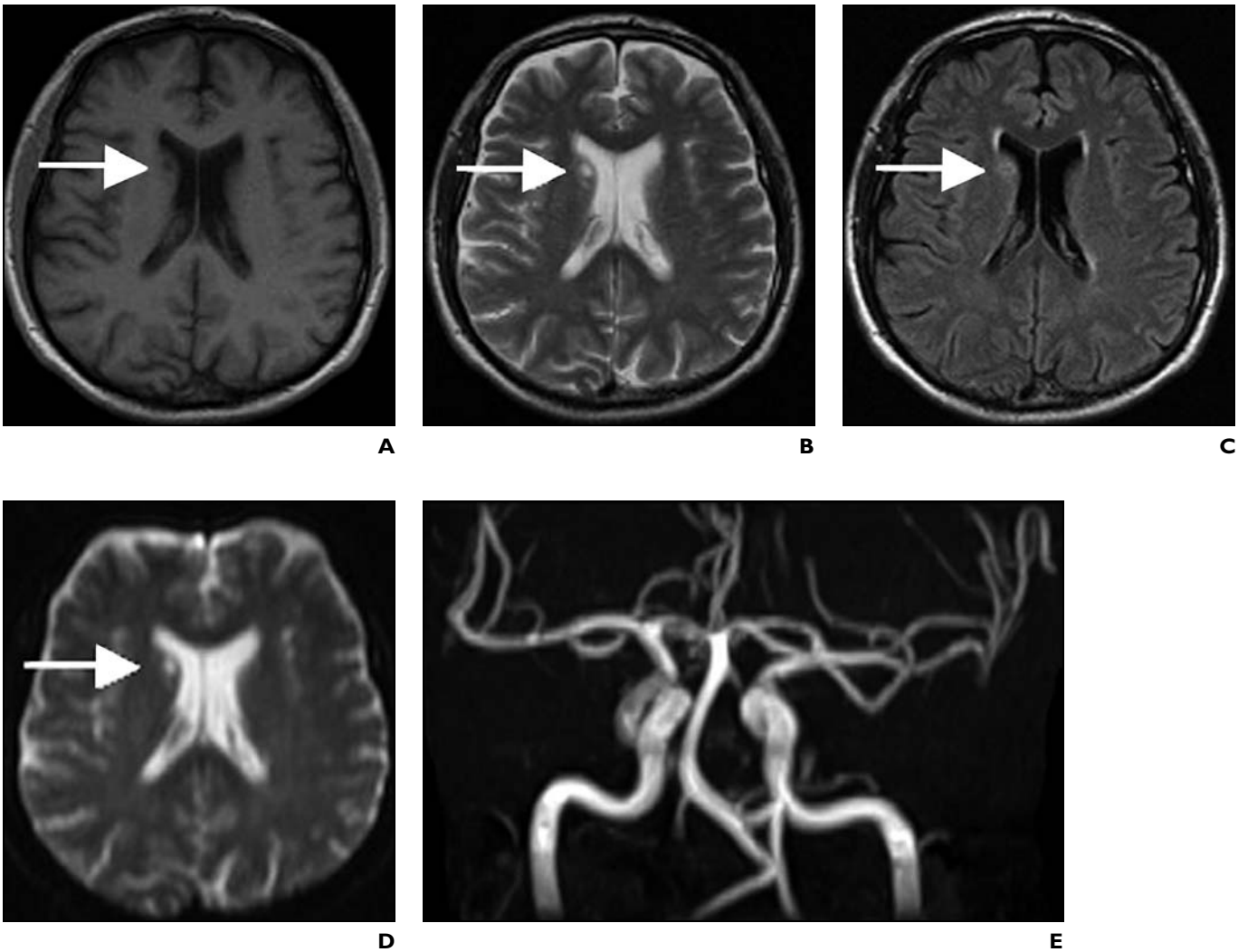

Fig. 6.—48-year-old man with no known risk factors for atherosclerosis.
A–D, T1-weighted (**A**), FLAIR (**B**), T2-weighted fast spin-echo (**C**), and diffusion-weighted (**D**) images show small lacunar infarction in right caudate nucleus (*arrows*).
E, Maximum-intensity-projection 3D time-of-flight angiogram shows normal findings for arterial system.

Colonic Disease

In all subjects, sufficient distention of all colonic parts was obtained. All images were of diagnostic quality, except for eight MR colonography components in which remaining stool hampered reliable diagnosis. Twelve examinations of the colon showed unequivocal polyps ranging in diameter from 5 to 13 mm (Fig. 9). Diverticular disease was diagnosed in 15 subjects, which was rated as a nonrelevant side finding.

Other Findings

Beyond the targeted organs (arteries, brain parenchyma, heart, colon), additional findings were reported, particularly in the abdomen. These findings are listed in Table 5. One renal cell carcinoma was detected, and no other malignancies were encountered.

Confirmation with Other Imaging Techniques

Seventy-five percent of all cases with relevant findings were corroborated clinically at the time of treatment (polypectomy, renal surgery) or by other dedicated forms of imaging including sonography, CT, and MRI (Tables 4 and 5). In one case, a contrast-enhancing 10-mm vertebral lesion, judged initially as relevant, was diagnosed as a hemangioma on dedicated spine MRI and hence was reclassified as not relevant. Of the nine pulmonary lesions identified on MRI, four were subsequently confirmed by MDCT in two subjects (Table 4); they were found to be partially calcified. All relevant arterial stenoses (except lower limb artery stenoses in one subject) were confirmed by sonography, regional MR angiography, or digital subtraction angiography. All colonic polyps were confirmed at colonoscopic polypectomy.

Image Demonstration

All subjects readily accepted the offer to have the imaging material shown to them after the examination, resulting in a high rate of compliance regarding diagnostic examinations or therapy for findings deemed relevant.

Discussion

Based on the latest high-performance gradients and a sliding-table concept, the outlined multiorgan MRI examination can be completed in a little more than 1 hr. All four components making up the examination are based on well-established and highly accurate protocols. Image quality was sufficient to readily detect abnormalities in the targeted organ systems (brain, heart, arteries, and colon) and surrounding tissues. The incidence of relevant findings in an asymptomatic population identified in both targeted and nontargeted organs was high and underscores the potential impact of an MRI-based screening strategy. Most of the relevant findings were confirmed by clinical examination, therapy, or further diagnostic workup.

Cardiovascular disease is the leading cause of mortality in western societies [21]. Although the known risk factors are readily identifiable by a combination of physical examination, laboratory analysis, and patient history, the proposed MRI protocol offers a unique opportunity to assess what damage if any has already been inflicted on the cardiovascular system. Thus, the outlined protocol has been shown to be highly sensitive regarding the identification of cerebrovascular disease. The size, number, and distribution of ischemic cerebral regions permit consideration of possible causes: thus, microangiopathic changes of the cerebral white matter are highly suggestive of hypertension [22], and thromboembolic changes are most frequently induced by high-grade carotid disease.

Early diagnosis of carotid stenoses is important because patients with stenoses of the internal carotid artery that are greater than 75%, as measured by Doppler examination, are at risk for stroke, in the range of 2% to 5%, within the first year of observation; this risk can be reduced by a factor of up to 55%. Furthermore, of patients who develop stroke during the observation of an asymptomatic lesion, 83% had no warning symptoms [23, 24]. Our 2.3% prevalence of cerebral infarction and microangiopathy correlates well with the literature [25], underlining the high sensitivity of MRI for intracerebral vascular lesions.

Because screening also must consider rare but significant cerebral tumors, a contrast-enhanced cerebral sequence should be part of the protocol. This sequence was integrated at

Fig. 7.—52-year-old man who is a heavy smoker. Maximum-intensity-projection image of upper thigh obtained from contrast-enhanced 3D gradient-echo MR angiography data set shows that left superior femoral artery has complex narrowing (*arrow*), which was shown to be focal dissection.

the end of the cardiac examination with no need for additional contrast agent administration because the sequence makes use of the contrast agent previously administered for MR angiography. Similarly, the proposed protocol offers a highly accurate assessment of myocardial viability. On the basis of delayed enhancement, infarcted myocardium is detected on T1-weighted images with high sensitivity and specificity [26, 27], allowing early secondary prevention strategies that have been shown to alter outcomes in high-risk, not yet symptomatic patients [28].

The cardiovascular screening component also encompasses a thorough analysis of the arterial lumen by means of intracerebral time-of-flight and contrast-enhanced multistation whole-body MR angiography. The quality of the former has been shown to be sufficient to detect small aneurysms or precursors thereof [29], as confirmed in two of the screened patients. Whole-body MR angiography mirrors the generalized nature of atherosclerotic disease from a diagnostic viewpoint. The 40-cm field of view of our scanner leads to a slight reduction in the signal-to-noise ratio at the upper and lower margins of the single source images, which is obvious in the maximum intensity projections; however, because the window and level settings can be adjusted for each of the subregions when multiplanar reformations are assessed, this lower signal-to-noise ratio does not result in problems. The technique has thus been shown to be accurate in the detection and characterization of arterial disease [13].

Early diagnosis of peripheral vascular disease plays a role in convincing patients to lower their risk profile and to extend physical activity [30]. Merely the lumen of the coro-

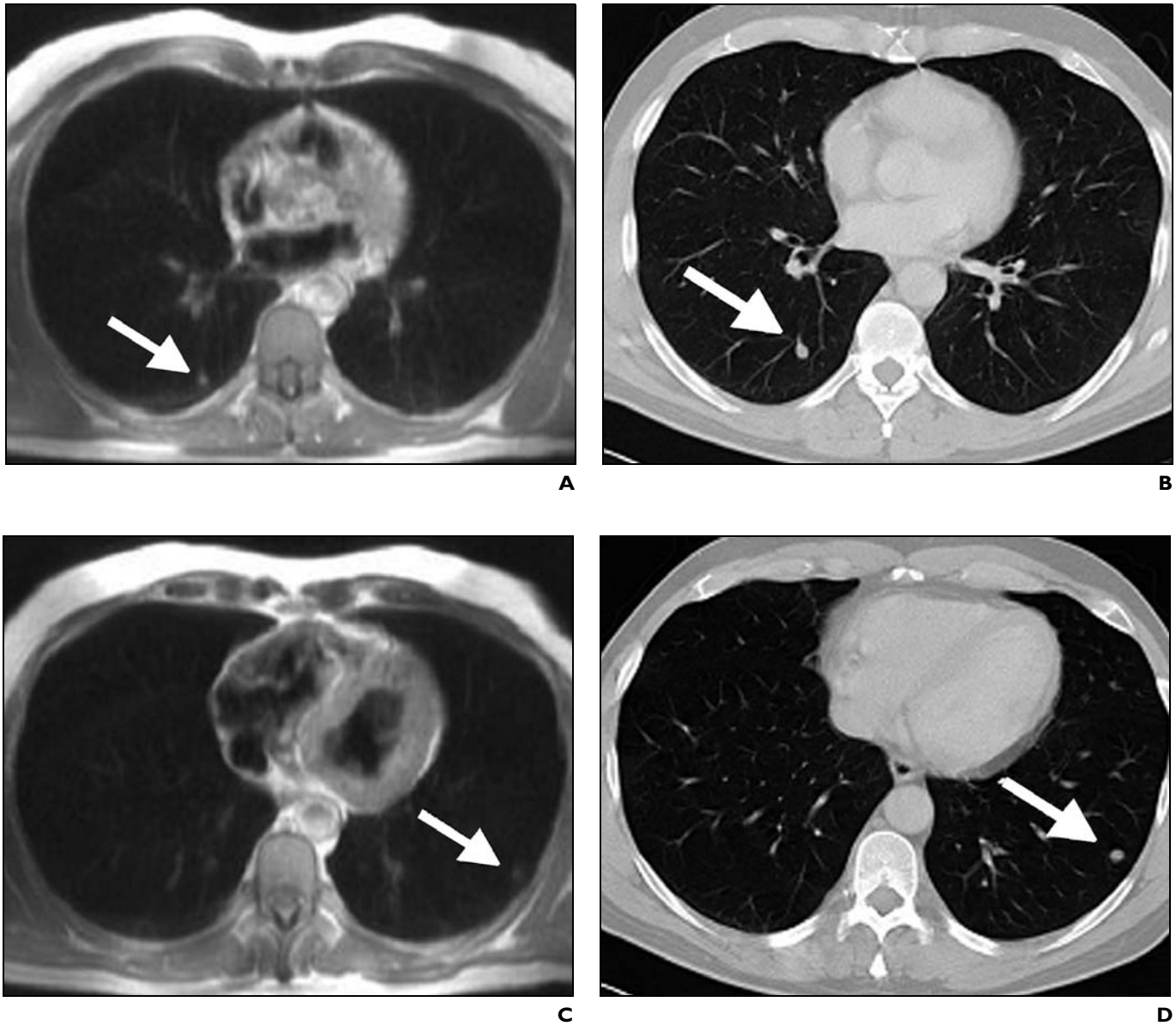

Fig. 8.—56-year-old male nonsmoker.
A–D, MR HASTE (**A** and **C**) and respective MDCT (**B** and **D**) images show benign partially calcified lesions in lower lobes (*arrows*).

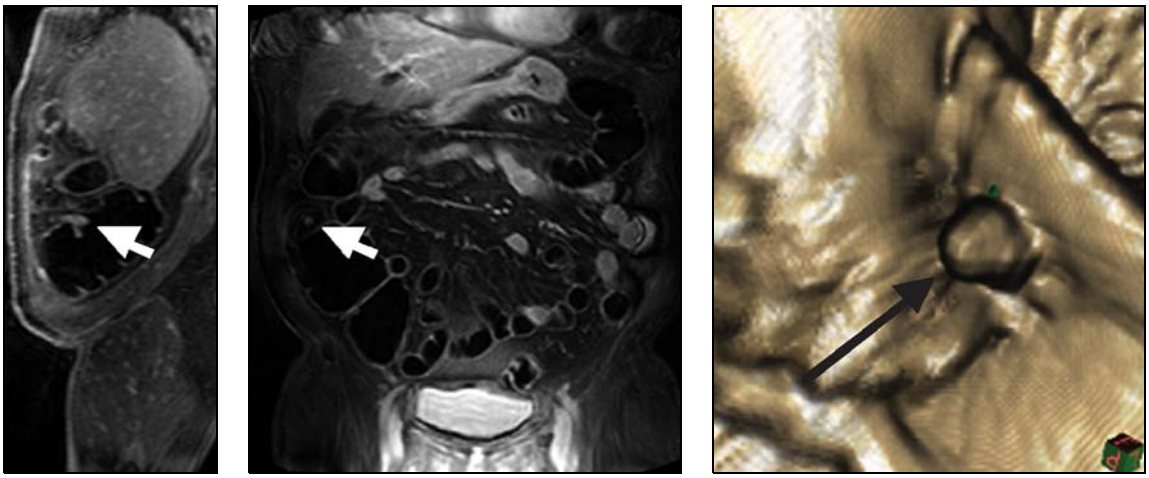

Fig. 9.—73-year-old man with history of polypectomy.
A and **B,** Sagittal reformation image (**A**) and coronal source image (**B**) of 3D gradient-echo data set show small polyp in ascending colon (*arrows*).
C, Endoscopic view also shows small polyp in ascending colon (*arrow*).

nary arteries remains unassessed by MR angiography. Even though several techniques have been proposed, none has gained clinical relevance. Although the ability to analyze myocardial viability in combination with ventricular function reduces the impact of this deficit, incorporation of coronary MR angiography into a future screening protocol remains highly desirable. Until this time, it seems crucial that some form of cardiac evaluation under stress conditions be performed.

As part of the cardiac examination, the lungs are also depicted and thus have to be assessed. MRI of the lung had been handicapped by susceptibility effects at the interfaces between the pulmonary interstitium and air-filled alveoli. These artifacts can be overcome using ultrashort TEs. On the basis of such sequences, the accuracy of MRI regarding the detection of pulmonary lesions has been shown to be quite high [31, 32]. In a study involving 30 patients with known pulmonary masses, axial HASTE images revealed 1,032 of 1,102 lesions seen on CT (Schroeder T et al., 2002 European Congress of Radiology). Reflecting the lack of signal-providing protons, smaller-calcified nodules were missed. Furthermore, lesions with a diameter of less than 3 mm were also missed. This might explain the low number of pulmonary lesions found in our study. Some kind of screening for pulmonary nodules should be performed in such a multiorgan MRI examination because lung carcinoma is the leading cause of cancer death and lesion detection at an early stage leads to a significantly higher number of T1 tumors found and consecutively to a better outcome [33].

Another focus of the proposed MRI-based screening protocol relates to the detection of colorectal cancer. Colorectal cancer has been a focus of screening efforts for quite some time. Despite these efforts, the incidence of colorectal cancer continues to increase with more than 130,000 newly diagnosed cases and 50,000 deaths in the United States alone [34]. The biology of colorectal cancer, evolving from precancerous colonic polyps to carcinoma over a considerable time span, has elevated colorectal polyp screening with subsequent endoscopic polypectomy to one of the most promising preventive measures in medicine [34, 35].

MR colonography overcomes many of the shortcomings limiting the clinical impact of existing screening techniques including the gold standard conventional colonoscopy. In the setting of a dark, water-filled colonic lumen, lesion detection is based on enhancement of the colonic wall and of colorectal masses [36]. The technique has been shown to be both sensitive and specific regarding the detection of colorectal masses [36, 37]. The overall prevalence of colonic polyps of 4% in our study population is lower than the expected prevalence of 14–25% [38] for patients older than 50 years. This result certainly might reflect the limited spatial image resolution, which does not permit the diagnosis of polyps less than 5 mm; however, it also mirrors the very low prevalence (< 1%) [39] of polyps in patients younger than 50 years. Just as important as diagnostic accuracy, high patient acceptance of the examination is assured by the lack of procedural pain and the prospect of fecal tagging, which has been shown to successfully eliminate the need for colonic cleansing [40].

Detected relevant findings were not limited to the target organs. Rather, there were a number of additional relevant findings. Analysis of the parenchymal organs in the abdomen can be based on 3D gradient-echo data sets collected in the arterial, portal venous, and hepatic venous phases. The first data set is provided as part of the whole-body MR angiography examination, and the subsequent data sets are collected for MR colonography. Previous studies have shown this type of dynamic contrast-enhanced 3D imaging of the abdomen to be accurate regarding the identification of abnormalities in the parenchymal organs [41]. Similar experiences have been reported on the basis of MR colonography data sets alone [37]. Hence, it was not surprising that the featured imaging protocol did result in the identification of multiple additional findings outside the target organs with considerable specificity.

Clearly, the limited number of individuals included in this study cannot provide relevant data regarding the value of MRI-based screening from a societal perspective. This will need to be accomplished in larger-scale studies. However, the presented data are sufficient to illustrate the technical feasibility of a comprehensive MRI-based screening approach capable of assessing multiple organ

systems in a single examination. Furthermore, this study does provide an overview of the kind of abnormalities that can be identified. The diagnostic accuracy of the different components making up the comprehensive MRI protocol has been established in a number of comparative examinations against gold standards. Lack of follow-up examinations in individuals lacking abnormal findings prohibits any meaningful analysis of the studied subjects in this regard.

On the basis of the available data, we are comfortable recommending therapeutic interventions or further diagnostic workup aimed at preventing disease progress. Furthermore, we found the images displaying abnormalities useful in persuading subjects to consider lowering their risk profile by quitting smoking, reducing cholesterol intake, or becoming more compliant with hypertension medication. Although this study falls short of offering conclusive evidence, immediate reactions of individuals at the time of image data presentation did indeed

TABLE 5 Findings Beyond the Target Diseases

Technique	Incidental Findings on MRI	Relevant Findings (*n*)	Confirmation of Relevant Findings	Nonrelevant Findings (*n*)
Cerebral MRI	Fenestration of basilar artery	1	Dedicated MRI	
	Temporal angioma	1	Dedicated MRI	
	Suspicion of small cerebral tumor	1	Dedicated MRI	
	Sinusitis	9	Clinical	32
	Opacification of mastoid cells	1	Clinical	3
	Aneurysm (size, 5 mm) of the anterior communicating artery	1	Dedicated CT	
	Cerebellar atrophy		Dedicated MRI	1
	Generalized atrophy	1	Dedicated MRI	
	Cyst in lenticular nucleus		Dedicated MRI	1
	Arachnoid cyst		Dedicated MRI	4
	Atheroma of skin		None	1
	Thalamic cavernoma	1	Dedicated MRI	
	Total	16		42
MR angiography	Lusoric artery	1	None	
	Adrenal adenoma	2	Dedicated MRI	
	Hemangioma	1	Dedicated MRI	
	Thyroid lesions or enlargement	4	Sonography	
	Gastric herniation	1	None	
	Doubled inferior vena cava		None	1
	Renal mass	1	Surgery	
	Pelvic ectopic kidney	1	None	
	Renal calculi	1	CT	
	Renal cyst		Dedicated MRI	6
	Retroaortal renal vein	2	None	
	Hepatic cyst		Dedicated MRI	2
	Posttraumatic lesion of lower limb		Dedicated MRI	1
	Disk herniation or degenerative spinal disease	1	Dedicated MRI	3
	Nonossifying fibroma of the tibia		Dedicated MRI	1
	Varicosis of lower limb		None	1
	Atrophic kidney	1	Sonography	
	Total	16		15
Pulmonary MRI	Pleural scars	2	CT	
Cardiac MRI	Valve abnormalities	11	Echocadiography	
	Left ventricular myocardial hypertrophy	17	Echocadiography	
	Total	28		

Note.—List of additional/side findings. Only one false-positive diagnosis results from all 298 MR examinations. Some subjects have more than one diagnosis. Some findings were visible in more than one examination part (i.e., gastric herniation). *n* = number of subjects with respective finding. (**Table 5 continues on next page**)

TABLE 5 Findings Beyond the Target Diseases (continued)

Technique	Incidental Findings on MRI	Relevant Findings (*n*)	Confirmation of Relevant Findings	Nonrelevant Findings (*n*)
MR colonography	Vertebral hemangiomas	6	Dedicated MRI: hemangiomas confirmed	
	Undetermined suspicious spinal lesion	1	Dedicated MRI: hemangioma not confirmed	
	Degenerative spine disease	9	None	23
	Spinal disk protrusion or herniation	5	Dedicated MRI	3
	Intraspinal neurinomas	1	Dedicated MRI	
	Pancreatic pseudocyst or postinflammatory lesion		Dedicated CT: confirmed (*n* = 2)	3
	Adrenal adenoma	2	Dedicated MRI (in- and out-of-phase): confirmed	
	Prostate hyperplasia	4	None	
	Doubled renal pelvic system	2	None	
	Myomatous uterus	3	None	
	Uterine focal lesion	2	Clinical	
	Pulmonary bulla	1	CT	
	Axial gastric herniation	6	None	
	Colonic diverticuli		None	15
	Postinflammatory or posttraumatic renal lesion		Clinical	2
	Cholecystolithiasis	4	Sonography	
	Gastroduodenal diverticle	1	None	
	Hepatic cysts		Dedicated MRI	42
	Focal nodular hyperplasia		Dedicated MRI	1
	Hepatic adenoma	1	Dedicated MRI	
	Umbilic hernia		None	1
	Hepatic hemangioma		Dedicated MRI	2
	Renal cysts	2 (complicated)	Dedicated MRI	67
	Renal calculi	1	CT	
	Splenic hemangioma or cyst		Dedicated MRI	3
	Intraperitoneal lymphdenopathia after enteritis		Clinical	1
	Retroaortal renal vein	3	None	
	Biliary duct dilatation		Dedicated MRI	1
	Reflux nephropathia	1	Clinical	
	Ovarian follicle on cysts		Clinical	2
	Reflux esophagitis	1	Clinical	
	Total	56		166

Note.—List of additional findings. Only one false-positive diagnosis results from all 298 MRI examinations. Some subjects have more than one diagnosis. Some findings were visible in more than one examination part (i.e., gastric herniation). *n* = number of subjects with respective finding.

suggest a profound impact. The high compliance rate of individuals with suggested subsequent diagnostic and therapeutic steps supports this observation.

This study is one of the first attempts to implement and evaluate a comprehensive MRI-based screening examination. Compared with the radiation exposure caused by CT, public health concern associated with MRI is minimal. Thus, exposure to MRI as a patient has never been associated with any harmful side effects [42]. Side effects may, however, be associated with the administration of paramagnetic contrast agents, which must be considered an integral part of the proposed examination. Although rare, anaphylactoid reactions may occur. Hence, individuals need to be monitored during the examination procedure. Only one subject showed a minor allergoid reaction in this study. On the other hand, nephrotoxicity, a worry with iodinated contrast agents, is of no concern [43].

Preparation of the colon was necessary for MR colonography, which is known to be the most unpleasant part of conventional colonoscopy [44]. Because the single subjects were keen to receive the MRI examination, none complained about bowel cleansing.

This study, however, does not provide data about the potential benefits or costs that would be gained or would have to be spent for subsequent diagnostic or therapeutic procedures. Also, the potential harm due to treat-

ment of false-positive findings cannot be addressed. This study was not designed to answer these difficult questions; rather, it presents a potential multiorgan screening design and reports about the range of diseases that one encounters in such a setting.

We conclude that the outlined MRI-based screening strategy encompassing the brain, the arterial system, the heart, and the colon was well tolerated and yielded relevant, unsuspected findings for a variety of organs. The presented data point toward an increased use of MRI for screening in the future. However, as long as the individual and socioeconomic impact are not known, screening examinations should be performed in a research setting, which would also help to collect performance and outcome data.

References

1. Kopp AF, Schroeder S, Baumbach A, et al. Noninvasive characterisation of coronary lesion morphology and composition by multislice CT: first results in comparison with intracoronary ultrasound. *Eur Radiol* 2001;11:1607–1611
2. Henschke CI, McCauley DI, Yankelevitz DF, et al. Early Lung Cancer Action Project: overall design and findings from baseline screening. *Lancet* 1999;354:99–105
3. Diederich S, Wormanns D, Semik M, et al. Screening for early lung cancer with low-dose spiral CT: prevalence in 817 asymptomatic smokers. *Radiology* 2002;222:773–778
4. Ellis JR, Gleeson FV. New concepts in lung cancer screening. *Curr Opin Pulm Med* 2002;8:270–274
5. Johnson CD, Dachman AH. CT colonography: the next colon screening examination? *Radiology* 2000;216:331–341
6. U.S. Food and Drug Administration Web site. Whole body scanning using computed tomography (CT). Available at: www.fda.gov/cdrh/ct/. Accessed November 22, 2004
7. Europa: European Commission on Energy. Available at: http://europa.eu.int/comm/energy/nuclear/radioprotection/doc/legislation/9743_en.pdf. Accessed November 22, 2004
8. Hirai T, Korogi Y, Ono K, et al. Prospective evaluation of suspected stenoocclusive disease of the intracranial artery: combined MR angiography and CT angiography compared with digital subtraction angiography. *AJNR* 2002;23:93–101
9. Herskovits EH, Itoh R, Melhem ER. Accuracy for detection of simulated lesions: comparison of fluid-attenuated inversion-recovery, proton density–weighted, and T2-weighted synthetic brain MR imaging. *AJR* 2001;176:1313–1318
10. Nederkoorn PJ, Mali WP, Eikelboom BC, et al. Preoperative diagnosis of carotid artery stenosis: accuracy of noninvasive testing. *Stroke* 2002;33:2003–2008
11. Korst MB, Joosten FB, Postma CT, Jager GJ, Krabbe JK, Barentsz JO. Accuracy of normal-dose contrast-enhanced MR angiography in assessing renal artery stenosis and accessory renal arteries. *AJR* 2000;174:629–634
12. Hany TF, Debatin JF, Leung DA, Pfammatter T. Evaluation of the aortoiliac and renal arteries: comparison of breath-hold, contrast-enhanced, three-dimensional MR angiography with conventional catheter angiography. *Radiology* 1997;204:357–362
13. Goyen M, Quick HH, Debatin JF, et al. Whole-body three-dimensional MR angiography with a rolling table platform: initial clinical experience. *Radiology* 2002;224:270–277
14. Friedrich MG, Schulz-Menger J, Poetsch T, Pilz B, Uhlich F, Dietz R. Quantification of valvular aortic stenosis by magnetic resonance imaging. *Am Heart J* 2002;144:329–334
15. Klein C, Nekolla SG, Bengel FM, et al. Assessment of myocardial viability with contrast-enhanced magnetic resonance imaging: comparison with positron emission tomography. *Circulation* 2002;105:162–167
16. Li F, Sone S, Maruyama Y, et al. Correlation between high-resolution computed tomographic, magnetic resonance and pathological findings in cases with non-cancerous but suspicious lung nodules. *Eur Radiol* 2000;10:1782–1791
17. Luboldt W, Bauerfeind P, Wildermuth S, Marincek B, Fried M, Debatin JF. Colonic masses: detection with MR colonography. *Radiology* 2000;216:383–388
18. Ruehm SG, Goyen M, Quick HH, et al. Whole-body MRA on a rolling table platform (Angio-SURF) [in German]. *Rofo Fortschr Geb Rontgenstr Neuen Bildgeb Verfahr* 2000;172:670–674
19. Vogler H, Platzek J, Schuhmann-Giampieri G, et al. Pre-clinical evaluation of gadobutrol: a new, neutral, extracellular contrast agent for magnetic resonance imaging. *Eur J Radiol* 1995;21:1–10
20. Goyen M, Lauenstein TC, Herborn CU, Debatin JF, Bosk S, Ruehm SG. 0.5 M Gd chelate (Magnevist) versus 1.0 M Gd chelate (Gadovist): dose-independent effect on image quality of pelvic three-dimensional MR-angiography. *J Magn Reson Imaging* 2001;14:602–607
21. Anderson KM, Wilson PWF, Odell PM, Kannel WB. An updated coronary risk profile: a statement for health professionals. *Circulation* 1991;83:356–362
22. Kim DE, Bae HJ, Lee SH, Kim H, Yoon BW, Roh JK. Gradient echo magnetic resonance imaging in the prediction of hemorrhagic vs ischemic stroke: a need for the consideration of the extent of leukoariosis. *Arch Neurol* 2002;59:425–429
23. Moore WS, Barnett HJM, Beebe HG, et al. Guidelines for carotid endarterectomy: a multidisciplinary consensus statement from the Ad Hoc Committee, American Heart Association. *Circulation* 1995;91:566–579
24. Chambers BR, Norris JW. The case against surgery for asymptomatic carotid stenosis. *Stroke* 1984;15:964–967
25. Tsushima Y, Tanizaki Y, Aoki J, Endo K. MR detection of microhemorrhages in neurologically healthy adults. *Neuroradiology* 2002 Jan; 44:31–36
26. Gerber BL, Lima JA, Garot J, Bluemke DA. Magnetic resonance imaging of myocardial infarct. *Top Magn Reson Imaging* 2000;11:372–382
27. Barkhausen J, Ruehm SG, Goyen M, Buck T, Laub G, Debatin JF. MR evaluation of ventricular function: true fast imaging with steady-state precession versus fast low-angle shot cine MR imaging: feasibility study. *Radiology* 2001;219:264–269
28. Tu K, Mamdani MM, Jacka RM, Forde NJ, Rothwell DM, Tu JV. The striking effect of the Heart Outcomes Prevention Evaluation (HOPE) on ramipril prescribing in Ontario. *Can Med Assoc J* 2003;168:553–557
29. Okahara M, Kiyosue H, Yamashita M, et al. Diagnostic accuracy of magnetic resonance angiography for cerebral aneurysms in correlation with 3D-digital subtraction angiographic images: a study of 133 aneurysms. *Stroke* 2002;33:1803–1808
30. Fowler B, Jamrozik K, Norman P, Allen Y, Wilkinson E. Improving maximum walking distance in early peripheral arterial disease: randomised controlled trial. *Aust J Physiother* 2002;48:269–275
31. Thompson BH, Stanford W. MR imaging of pulmonary and mediastinal malignancies. *Magn Reson Imaging Clin N Am* 2000;8:729–739
32. Chung MH, Lee HG, Kwon SS, Park SH. MR imaging of solitary pulmonary lesions: emphasis on tuberculomas and comparison with tumors. *J Magn Reson Imaging* 2000;11:629–637
33. Flehinger BJ, Kimmel M, Melamed MR. The effect of surgical treatment on survival from early lung cancer. *Chest* 1992;101:1013–1018
34. Landis SH, Murray T, Bodden S, Wingo PA. Cancer statistics, 1998. *CA Cancer J Clin* 1998;48:6–29
35. Liebermann DA, Smith FW. Screening for colon malignancy with colonoscopy. *Am J Gastroenterol* 1991;86:946–951
36. Lauenstein TC, Debatin JF. Magnetic resonance colonography for colorectal cancer screening. *Semin Ultrasound CT MR* 2001;22:443–453
37. Luboldt W, Bauerfeind P, Steiner P, Fried M, Krestin GP, Debatin J. Preliminary assessment of three-dimensional magnetic resonance imaging for various colonic disorders. *Lancet* 1997;349:1288–1291
38. Neugut AI, Jacobson JS, Rella VA. Prevalence and incidence of colorectal adenomas and cancer in asymptomatic persons. *Gastrointest Endosc Clin N Am* 1997;7:387–399
39. Ang YS, Macaleenan N, Mahmud N, Keeling PW, Kelleher DP, Weir DG. The yield of colonoscopy in average-risk patients with non-specific colonic symptoms. *Eur J Gastroenterol Hepatol* 2002;14:1073–1077
40. Lauenstein TC, Goehde SC, Ruehm SG, Holtmann G, Debatin JF. MR colonography with barium-based fecal tagging: initial clinical experience. *Radiology* 2002;223:248–254
41. Hawighorst H, Schoenberg SO, Knopp MV, Essig M, Miltner P, van Kaick G. Hepatic lesions: morphologic and functional characterization with multiphase breath-hold 3D gadolinium-enhanced MR angiography—initial results. *Radiology* 1999;210:89–96
42. Ahmed S, Shellock FG. Magnetic resonance imaging safety: implications for cardiovascular patients. *J Cardiovasc Magn Reson* 2001;3:171–182
43. Prince MR, Arnoldus C, Frisoli JK. Nephrotoxicity of high-dose gadolinium compared with iodinated contrast. *J Magn Reson Imaging* 1996;6:162–166
44. Lieberman D. Colon cancer screening: beyond efficacy. *Gastroenterology* 1994;106:803–807